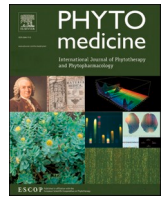




Since January 2020 Elsevier has created a COVID-19 resource centre with free information in English and Mandarin on the novel coronavirus COVID-19. The COVID-19 resource centre is hosted on Elsevier Connect, the company's public news and information website.

Elsevier hereby grants permission to make all its COVID-19-related research that is available on the COVID-19 resource centre - including this research content - immediately available in PubMed Central and other publicly funded repositories, such as the WHO COVID database with rights for unrestricted research re-use and analyses in any form or by any means with acknowledgement of the original source. These permissions are granted for free by Elsevier for as long as the COVID-19 resource centre remains active.



## Original Article

## Dehydrozingerone ameliorates Lipopolysaccharide induced acute respiratory distress syndrome by inhibiting cytokine storm, oxidative stress via modulating the MAPK/NF- $\kappa$ B pathway

Satya Krishna Tirunavalli<sup>a,c,1</sup>, Karthik Gourishetti<sup>a,1</sup>, Rama Satya Sri Kotipalli<sup>a</sup>, Madusudhana Kuncha<sup>a</sup>, Muralidharan Kathirvel<sup>a</sup>, Rajwinder Kaur<sup>a</sup>, Mahesh Kumar Jerald<sup>b</sup>, Ramakrishna Sistla<sup>a,c,\*</sup>, Sai Balaji Andugulapati<sup>a,c,\*</sup>

<sup>a</sup> CSIR-Indian Institute of Chemical Technology (IICT), Hyderabad 500 007, India

<sup>b</sup> CSIR - Centre for Cellular & Molecular Biology (CCMB), Hyderabad 500 007, India

<sup>c</sup> Centre for Academy of Scientific and Innovative Research (AcSIR), CSIR-Indian Institute of Chemical Technology (CSIR-IICT), Hyderabad, India

## ARTICLE INFO

## Keywords:

ARDS  
Lung injury  
Dehydrozingerone  
Elastase  
MAPKinase  
NF- $\kappa$ B

## ABSTRACT

**Background:** Inflammation-mediated lung injury is a major cause of health problems in many countries and has been the leading cause of morbidity/mortality in intensive care units. In the current COVID-19 pandemic, the majority of the patients experienced serious pneumonia resulting from inflammation (Acute respiratory distress syndrome/ARDS). Pathogenic infections cause cytokine release syndrome (CRS) by hyperactivation of immune cells, which in turn release excessive cytokines causing ARDS. Currently, there are no standard therapies for viral, bacterial or pathogen-mediated CRS.

**Purpose:** This study aimed to investigate and validate the protective effects of Dehydrozingerone (DHZ) against LPS induced lung cell injury by *in-vitro* and *in-vivo* models and to gain insights into the molecular mechanisms that mediate these therapeutic effects.

**Methods:** The therapeutic activity of DHZ was determined in *in-vitro* models by pre-treating the cells with DHZ and exposed to LPS to stimulate the inflammatory cascade of events. We analysed the effect of DHZ on LPS induced inflammatory cytokines, chemokines and cell damage markers expression/levels using various cell lines. We performed gene expression, ELISA, and western blot analysis to elucidate the effect of DHZ on inflammation and its modulation of MAPK and NF- $\kappa$ B pathways. Further, the prophylactic and therapeutic effect of DHZ was evaluated against the LPS induced ARDS model in rats.

**Results:** DHZ significantly ( $p < 0.01$ ) attenuated the LPS induced ROS, inflammatory cytokine, chemokine gene expression and protein release in macrophages. Similarly, DHZ treatment protected the lung epithelial and endothelial cells by mitigating the LPS induced inflammatory events in a dose-dependent manner. *In vivo* analysis showed that DHZ treatment significantly ( $p < 0.001$ ) mitigated the LPS induced ARDS pathophysiology of increase in the inflammatory cells in BALF, inflammatory cytokine and chemokines in lung tissues. LPS stimulated neutrophil-mediated events, apoptosis, alveolar wall thickening and alveolar inflammation were profoundly reduced by DHZ treatment in a rat model.

**Conclusion:** This study demonstrates for the first time that DHZ has the potential to ameliorate LPS induced ARDS by inhibiting cytokine storm and oxidative through modulating the MAPK and NF- $\kappa$ B pathways. This data provides pre-clinical support to develop DHZ as a potential therapeutic agent against ARDS.

**Abbreviations:** ALP, alkaline phosphatase; ARDS, acute respiratory distress syndrome; BALF, bronchoalveolar lavage fluid (BALF); COVID-19, coronavirus diseases 2019; CRS, Cytokine Release Syndrome; DHZ, dehydrozingerone; hr, hour; LDH, lactic acid dehydrogenase; LPS, lipopolysaccharide; MPO, myeloperoxidase; NE, neutrophil elastase; ROS, reactive oxygen species; RT-qPCR, reverse transcriptase quantitative PCR; SRB, sulforhodamine-B.

\* Corresponding authors.

E-mail address: [balaji@iict.res.in](mailto:balaji@iict.res.in) (S.B. Andugulapati).

<sup>1</sup> Equal first authors.

<https://doi.org/10.1016/j.phymed.2021.153729>

Received 31 May 2021; Received in revised form 12 August 2021; Accepted 23 August 2021

Available online 27 August 2021

0944-7113/© 2021 Elsevier GmbH. All rights reserved.

## Background

To meet the unmet medical need for patients suffering from lung inflammation/acute lung injury, we developed *in-vitro* and *in-vivo* models. These models exactly mimic inflammatory/damage conditions in *in-vitro* models and causes severe ARDS in animals as evidenced by increased inflammatory-cell infiltration/markers expression and pathological changes in lungs.

### Translational Significance

Developing drugs against lung inflammation highly warranted and may significantly increase the survival of patients (especially COVID-19 patients). Our pre-clinical studies demonstrated that, dehydrozingerone significantly mitigates the LPS induced ARDS by modulating the MAPK/NF- $\kappa$ B pathway. Dehydrozingerone may be a potential drug to treat bacterial or viral induced lung inflammation/cytokine storm.

## Introduction

Lung inflammation or injury is a critical disorder characterized by acute hypoxemic respiratory failure with an underlying cause of hyperimmunity, oxidative stress, cytokine storm, and injury of epithelial and endothelial cells (Amani et al., 2021). Bacterial or viral infections rank as the top etiology of Acute lung injury (ALI) in intensive care units (Erickson et al., 2007). Previous studies reported that several bacterial strains such as *Streptococcus pneumoniae*, *Haemophilus influenzae*, *Staphylococcus aureus* cause severe respiratory tract infections (Bosch et al., 2013). Notably, viruses such as a respiratory syncytial virus (RSV), human parainfluenza viruses type 1, 2, and 3, adenoviruses (ADV) influenza viruses type A and B, and human metapneumoviruses (HMPV) are most frequently detected in children with acute respiratory infections. Severe acute respiratory syndrome (SARS) virus, influenza virus H1N1, H9N2 Middle East respiratory syndrome (MERS) and recent SARS-CoV-2 might even induce deadly ALI and ARDS in middle and old age people.

ARDS is a typical condition with intense inflammatory damage of alveolar cells and capillary membrane causing high permeability and infiltration of immune cells in lungs resulting in decreased oxygenation (Silva et al., 2020). ARDS is developed by either direct affronts to the lung epithelium (pulmonary ARDS) or indirect insults to the vascular endothelium secondary to an acute systemic inflammatory response (extrapulmonary ARDS). The most typical cause of pulmonary ARDS is bacterial infections such as pneumonia, whereas extrapulmonary ARDS is mostly caused by sepsis. In both cases, activation and infiltration of inflammatory cells cause an imbalance in pro-inflammatory and anti-inflammatory cytokine levels (also termed as cytokine storm) leading to severe morbidity and mortality.

An epidemiological data suggests that there are 18–79 ARDS cases per one hundred thousand persons per year, however, in the current pandemic conditions, these numbers were increased tremendously (Rubinfeld et al., 2005). It was reported that COVID-19 patients present primarily fever, myalgia or fatigue and dry cough, whereas the patients with severe illness develop dyspnea and hypoxemia within 1 week after onset of the disease, which rapidly progresses to acute lung injury or ARDS (Hung et al., 2020). Further, acute lung injury or ARDS causes hyper-inflammation, followed by cytokine storm and lung damage as observed in SARS-CoV-2 patients.

In lung injury, macrophages play a major role in the initiation of inflammation by releasing several cytokines and chemokines which lead to the activation and recruitment of neutrophils and other inflammatory

cells (Andonegui et al., 2009). Neutrophil activation increases their ability to adhere, role and emigrate through the endothelium. Along the same line, the endothelial cells also show increased expression of adhesion molecules to allow neutrophils to cross and invade the alveolar epithelium LPS activated epithelial cells produce inflammatory factors, promote systemic/ local reactions and cellular damage by communicating the signals to endothelial cells to resulting ARDS. Along with the association of cells and their responses, regulating the release of ROS, cytokines from inflammatory cells and controlling the airway epithelial cells/endothelial cells damage could be a potential target for discovering and developing novel therapeutic drugs against ARDS.

Hence discovering a novel therapeutic drug for ARDS has become a priority in the current pandemic situation. To screen drugs against lung inflammation, LPS inflammation models have been using as they activate TLR-4 receptor and causes activation of TNF- $\alpha$ , MIP1- $\alpha$ , IL-10, IL-1 $\beta$ , IL-12p40, IL8 and other markers in macrophages or inflammatory cells by inducing the acquired immune system. The pathologic abnormalities in the acute phase of pulmonary infections include a diffused alveolar damage, involving disruption and loss of both epithelial and endothelial cells and exudation of protein-rich fluid.

It was reported that culture of normal lung epithelial cells (BEAS-2B) with inflammatory cytokines such as TNF- $\alpha$  or IL-1 $\beta$  was found to enhance ICAM-1 expression and induce de-novo VCAM-1 expression. As the activation of ICAM-1 and VCAM-1 are involved in the damage of epithelium (Kim et al., 2014), attenuation of these adhesion molecules may play a role in protecting the lungs against infections. Therefore, a potential pharmacological lead compound not only to be screened using macrophages/inflammatory cells but also in normal-lung epithelial and endothelial cells.

Phytochemicals are potential candidates for anti-bacterial, anti-viral, anti-inflammatory, antioxidant and anti-cancer therapeutics. For example, curcumin a well-studied phytochemical has been shown to have its biological activity in inflammation and cancer treatment (Yogosawa et al., 2012). However, curcumin has certain limitations to its pharmacological effects, such as poor solubility and bioavailability. In the present investigation, we have evaluated Dehydrozingerone (DHZ-a curcumin analogue) for its anti-inflammatory activity in lung infections. DHZ is a phenolic compound derived from ginger (*Zingiber officinale*) rhizomes previously shown to possess anti-inflammatory and antioxidant activities (Chibber et al., 2020). The therapeutic effects of DHZ against pulmonary cytokine release syndrome caused by pathogens such as bacteria or viruses are not explored. In the current study, we investigated the anti-inflammatory and antioxidant activity of DHZ using mouse macrophages RAW 264.7, human lung epithelial cells BEAS-2B and endothelial cells *in vitro* models for cytokine production and cellular damage. Using the *in vivo* cytokine release syndrome model developed in rats (intratracheal administration of LPS), we have observed a great therapeutic potential of DHZ as an anti-inflammatory agent and its activity depends on modulating the NF- $\kappa$ B/MAPK pathway.

## Materials and methods

### Materials

Dehydrozingerone (> 99% purity) bought from TCI chemicals and structure of the compound was shown in Fig. S1A, Lipopolysaccharide (LPS from *E. Coli* 055: B5) purchased from Sigma Aldrich (USA). Dexamethasone was purchased from Sigma-Aldrich, USA. C-DNA synthesis kit, SYBR green mix purchased from Takara bioscience INDIA. Antibodies GAPDH, JNK P-JNK, c-JUN, p-NF- $\kappa$ B, NF- $\kappa$ B, p38, pP38, Histone-H3, I $\kappa$ B, p-I $\kappa$ B, MPO, Neutrophil Elastase were purchased from Cell signalling technology (USA), ELISA kits (IL-6, CCL2, IL-10, INF- $\gamma$ ,

Human-IL-8 and IL-1 $\beta$  were bought from R&D systems. Human IL-6 ELISA kit was procured from Elabsciences (Houston, USA). Secondary Antibodies were procured from Jackson Immuno research private limited (USA). TUNEL kit was procured from Merk Millipore.

#### Cell lines and culture conditions

To mimic disease conditions BEAS-2B, HUVEC and RAW-264.7 cell lines were used, and these cell lines were procured from ATCC, BEAS-2B (human bronchial epithelial cell line-2B) cultured in BEGM media with growth factor supplements (LONZA, USA). Human umbilical vein endothelial cells (HUVEC) were cultured in EBM media with growth factor supplements (LONZA, USA). RAW 264.7 cells were cultured in Dulbecco's modified Eagle's medium with 4 mM L-glutamine, 3.7 g/l sodium bicarbonate, 4.5 g/l glucose, and 10% fetal bovine serum. All the cells were maintained in a humidified atmosphere of 95% air with 5% CO<sub>2</sub> at 37 °C. All experiments were performed at 70-90% confluence and between 3-6 passages. All *in vitro* experiments were conducted 3-4 times as biological repeats and three times as technical repeats.

#### Treatment conditions for LPS induced cytokine releases/ cell injury experiments

RAW 264.7 cells or BEAS-2B or HUVEC cells were cultured in specified media and were seeded in 60 mm dishes ( $4 \times 10^5$  cells/dish). After 24 h of attachment, cells were washed with serum-free media and incubated for another 6 h in a serum-free medium. Thereafter, cells were pre-treated with DHZ in 3 concentrations (12.5, 25 and 50  $\mu$ M) for 2 h, then cells were stimulated with LPS (5  $\mu$ g/ml for BEAS-2B cells and 1  $\mu$ g/ml for RAW-264.7 and HUVEC cells) and further incubated for 12 h, thereafter, cell supernatant was collected for ELISA and cells were harvested for gene expression analysis or western-blot analysis or DCFDA analysis.

#### Cell viability by SRB assay

Cell viability was performed by SRB assay as per previous literature with minor modifications (Andugulapati et al., 2020b). Briefly,  $8 \times 10^3$  cells/well were seeded in a 96 well plate after 18 h of post-seeding, cells were treated with 0.1%-DMSO (vehicle control) or DHZ at various concentrations (500, 250, 125, 62.5, 31.25, 15.65 and 7.7  $\mu$ M) in the presence or absence of LPS for 48 h. After treatment, cells were fixed with 10% Trichloro Acetic Acid (TCA), stained with 0.057% (W/V in 1% Acetic Acid) SRB and washed with 1% acetic acid then bound dye was dissolved with 10mM tris-base and absorbance was measured at 562 nm. IC<sub>50</sub> values were calculated using the curve-fit method by GraphPad Prism-5.

#### Gene expression analysis

RNA isolation was carried out using RNAiso plus as described earlier (Balaji et al., 2016). Briefly, RNA was isolated using the trizol-chloroform method and total RNA was quantified using nano-drop. cDNA synthesis was performed using 1  $\mu$ g of RNA with prime script cDNA synthesis kit (Takara bio-India) according to manufacturer's instructions. Primers for pro-inflammatory cytokines (IL-6, IL-1 $\beta$ , TNF- $\alpha$ , F4/80 and IL-8/CXCL-1) markers, chemokine markers (CCL2, CCL3, CCL7, CXCL7, CXCL-8/MIP-2 and CXCL11), anti-inflammatory marker (IL-10), alveolar pulmonary stretch (amphiregulin), epithelial cell damage (club cell protein 16 [CC16]), and endothelial cell damage (intercellular adhesion molecule [ICAM]-1, vascular cell adhesion molecule-1 [VCAM-1]), and reference markers (*GAPDH*,  $\beta$ 2M and  $\beta$ -actin) were designed using Primer-3 software and respective sequences were shown in Tables S1 and S2. Reverse transcription-quantitative PCR (RT-qPCR) was carried out using SYBR green mix (DSS, Takara BIO) and the relative expression of mRNA was calculated using the comparative

Ct ( $\Delta$ Ct) and data were expressed as Mean  $\pm$  SEM.

#### ROS estimation by DCFDA assay

RAW 264.7 cells/BEAS-2B cells were seeded in 12 well plate ( $2 \times 10^5$  cells/well), after 24 h of attachment, cells were washed with PBS and incubated with serum-free media for 6 h. Then cells were pre-treated with specified concentrations of DHZ for 2h, thereafter cells were stimulated with LPS for another 12 h. Then cells were washed with PBS and 1  $\mu$ g/ml of DCFDA was added and incubated for 30 min in 37 °C incubator (Tetz et al., 2013). After incubation, cells were trypsinized, washed with PBS and were analysed by BD-Accuri® C6 flow cytometer for measuring the mean fluorescence intensity of DCFDA.

#### Western-blot analysis

Cell or tissue homogenates were subjected to protein isolation using RIPA lysis buffer, and then protein concentrations were estimated using bicinchoninic acid reagent (BCA-kit from Thermo Scientific, USA). An equal amount of (30  $\mu$ g) protein from all samples were loaded into SDS-PAGE Bis-Tris 8–10% protein gel for electrophoresis and then transferred onto polyvinylidene difluoride (PVDF) membranes (0.45  $\mu$ m, Millipore, Billerica, MA, USA). After protein transfer, PVDF membranes were blocked with 5% Bovine serum albumin (Sigma Aldrich, USA) for 1 h at room temperature and then blots were incubated with primary antibodies overnight at 4 °C. Primary antibodies (phospho-NF $\kappa$ B, total NF $\kappa$ B, phospho NF $\kappa$ B, p38, phospho p38, c-JUN) and loading control antibody GAPDH were purchased from Cell signalling technology, Massachusetts, USA. Secondary antibodies (Jackson Laboratory, USA) and an ECL kit (Advansta, Menlo park, CA, USA) were employed to generate chemiluminescent signals. ReBlot Plus Strong Antibody Stripping Solution (Millipore, USA) was used to re-probe the blots. All immunoblot quantifications were representing the triplicate repeats. Densitometry analysis was performed using ImageJ software.

#### Experimental animals and induction of ARDS in male SD rats by intra-tracheal instillation of LPS

Adult male SD rats (200–230 g, n = 50) at 8-10 weeks were used to develop LPS induced ARDS. Animals were acclimatized at 24–26 °C and were maintained in 12 h dark and 12 h light cycle and animals had free access to a normal chow diet and water ad libitum. Animal experimental protocol was reviewed by Institutional Animal Ethics Committee (IAEC) and approved on 18 July 2020 (Registration no: IICT/017/2020), CSIR-Indian Institute of Chemical Technology. All animal experiments were performed as per the guidelines of the Committee for the Purpose of Control and Supervision on Experiments on Animals (CPCSEA). LPS (5 mg/kg) induced ARDS/lung Injury is the standard model for establishing the therapeutic model of ARDS in rats. Since LPS induced ARDS is an acute model, we used 12 h and 24 h endpoints for measuring the efficacy of DHZ. Based on the pilot experiment, we have selected the doses for the *in vivo* study. Male SD rats were randomly assigned into 8 groups (n = 9/group) and named as sham control 1 (for 12 h time point), sham control-2 (for 24 h time point), LPS-12 h (disease control for 12 h), LPS + DHZ-25 mg/kg-12h, LPS + DHZ-50 mg/kg-12 h, LPS-24 h (disease control for 24 h), LPS + DHZ-25 mg/kg-24 h, and LPS + DHZ-50 mg/kg-24 h. LPS was dissolved in PBS to attain the concentration of 5mg/ml. LPS was administered intratracheally (5 mg/kg) to the anesthetized (ketamine (80 mg/kg) and xylazine (10 mg/kg)) SD rats and then allowed them for recovery (Andugulapati et al., 2020a). After 2 h of LPS administration, rats were treated with DHZ- 25 mg/kg and 50 mg/kg for 12 h and 24 h in both sets. After LPS instillation (12 h/24 h), blood samples were collected for cytology in 12 h set and then BALF samples were collected and a portion of BALF samples were subjected to cytology and ALP/LDH estimations, remaining part was centrifuged and stored in -80 °C for further analysis. Animals were sacrificed, right lungs were

collected for histopathological examination, while left lungs were collected for wet-to-dry (W/D) analysis, western blotting and RT-qPCR analysis.

#### Lung wet-dry weight (W/D) ratio

After sacrificing the animals, lung tissues (left lung tissue) from 4 rats per group which are not subjected to BALF (Bronchoalveolar Lavage Fluid) collection were excised. The surface liquid of the lung section was drained with clean filter paper carefully and then record as the wet weight. Then lung tissues were exposed to 80 °C for 48 h then the dry weight was obtained. The W/D ratio was calculated to evaluate the moisture content of lung tissue.

#### BALF analysis

BALF was collected by cannulating the trachea in an anaesthetized (Pentobarbital-50 mg/kg) animal, a volume of 3 ml sterile saline was slowly infused into the rat lungs and collected 2 ml of BALF. Then, BALF was centrifuged at 2000 rpm at 4 °C for 10 min, then cell pellets were re-suspended in 500 µl of sterile saline to quantify inflammatory cells and BALF supernatant was examined for ALP and LDH parameters using the auto-analyzer (Siemens, Germany).

#### Cytokine analysis using ELISA

Cytokine (IL-6, IL-8, CCL2, IL-1 $\beta$ , IFN  $\gamma$  and IL-10) levels were estimated in cell culture-supernatants, BALF and lung tissue homogenates by using ELISA kits as per the manufacturer's instructions. Briefly, Samples and standards were pipetted into a micro-plate pre-coated with capture antibodies and incubated at room temperature for 2 h. After washing 3 times with wash buffer, biotinylated detection antibodies were added and incubated for 1hr at room temperature, followed by incubation with avidin horseradish peroxidase (HRP) conjugate for 30 min. Then substrate solution was added and incubated the plates at room temperature in the dark for 15 min. The reaction was stopped by the addition of 1 M H<sub>2</sub>SO<sub>4</sub> and the optical density of each well was measured at 450 nm with a micro-plate reader (Synergy 5, BioTek Instruments, USA).

#### Nitric oxide estimation (modified Griess assay)

Lung tissues were homogenized and centrifuged in ice-cold condition at 12,000 rpm for 12 min and then supernatants were collected and used immediately to measure nitric oxide (NO) levels. Griess reagent was used to evaluate the nitrate levels (NO) of the samples by mixing an equal proportion of both Griess reagent and supernatants of the lung tissue samples, incubated for 10 min in dark at 37 °C, and absorbance was measured at 548 nm. Data obtained from the experiments were normalized using protein content and expressed as µM/mg of tissue.

#### Histopathology and immunohistochemistry

A portion of the pulmonary lobe was collected, rinsed with ice-cold phosphate buffer saline, and fixed with 10% neutral-buffered formalin, embedded in paraffin wax, sectioned (4 µm), stained with H&E and few sections were taken on positively charged slides for immunohistochemistry analysis. The slides were analysed with a microscope in a random order using a (10 ×) objective. The severity of the lung injury and edema in alveolitis were observed using H&E staining and were semi-quantitatively assessed by a pathologist in a blinded fashion. The inflammation/lung injury of the tissue was assessed by measuring the accumulation of neutrophils in the alveolar or the interstitial space, alveolar inflammation, wall thickening, oedema, fibrosis or peri bronchitis, peri arteriolar inflammation with infiltration of inflammatory cells and thickening of the alveolar wall.

Immunohistochemistry was performed as described in the previous protocol (Liu et al., 2018). In- brief, tissue sections were incubated with primary antibodies (Neutrophil-elastase Thermo-scientific, USA and myeloperoxidase (Abcam, USA)) overnight. Then sections were washed and stained with secondary anti-rabbit antibody tagged with horse-radish peroxidase (HRP) enzyme (Jakson Laboratory, USA) on the following day protein expression was detected using SignalStain® DAB Chromogen kit (Cell Signaling Technology, USA). The number of positive cells for specified antibodies were calculated per mm<sup>2</sup> of the specimen and plotted the graphs for better representation of the results.

#### Statistical analysis

All results are expressed as mean  $\pm$  standard error of the mean (SEM) and analysed with the GraphPad Prism 5.0 software. All data were analysed by one-way or two-way ANOVA with multiple comparisons or Student t-test where appropriate. In all cases,  $p < 0.05$  was considered statistically significant.

#### Results

##### DHZ treatment attenuates the LPS induced IL-6 gene expression in macrophages

It was reported that IL-6 levels are elevated in the BALF of patients who are at risk for ARDS and it remains elevated throughout the development of ARDS (Liu et al., 2020). We have investigated the DHZ efficacy towards IL-6 gene expression and protein release using mouse macrophage cell line RAW264.7. Before investigating the effect of DHZ on mRNA levels of cytokines, cytotoxicity assay was performed and data reveals that DHZ did not show any cell death in the presence or absence of LPS (1 µg/ml) up to 70 µM and IC<sub>50</sub> of DHZ was found to be 104 µM (Fig. S1B–D). Based on these results 12.5, 25 and 50 µM concentrations were selected for further analysis.

LPS stimulation increased the mRNA and protein levels of IL-6 in several folds as observed by qRT-PCR and ELISA analysis when compared to the control (Fig. 1A and B). To compare the effect of DHZ with a standard anti-inflammatory drugs, cells were pre-treated with DHZ or Dexamethasone (DEXA) before LPS stimulation. Interestingly, our results revealed that treatment with DHZ significantly mitigated the IL-6 mRNA levels in a dose-dependent manner and showed equal potency as DEXA (Fig. 1D). Further, DHZ and DEXA showed a significant reduction in IL-6 protein levels analysed by ELISA, similar to the gene expression data (Fig. 1C).

We have extended our analysis to determine the effect of DHZ on other major LPS induced inflammatory cytokines and chemokines in RAW264.7 cells (Fig. 1E–L). It was found that the key cytokines (TNF- $\alpha$ , and IL- $\beta$ ), chemokines (CXCL-8/MIP-2, CXCL-11, CCL2, and CCL7), and inflammatory markers (COX-2 and F4/80) were highly upregulated upon LPS stimulation (Fig 1E–L). DHZ treatment showed a significant reduction in TNF- $\alpha$  and IL-1 $\beta$  expression levels comparable to DEXA-100 ng/ml (Fig. 1E and F). Further, DHZ significantly reduced the expression levels of chemokines, Cox-2 and F4/80 in dose-dependent manner. Altogether, these results clearly demonstrate that DHZ functions as an anti-inflammatory agent in macrophage cells.

##### DHZ reduces the inflammatory cytokine levels in epithelial and endothelial cells

It is still unclear how the inflammatory cascades orchestrate the lung damage by involving the immune cell infiltration (for example macrophages, neutrophils, etc.), epithelial and endothelial cell damage markers in ARDS (Salgado et al., 1994). However, the pathogen-induced lung injury in ARDS has been shown to involve inflammatory signalling activation not only in the immune cells (macrophages) but also in epithelial and endothelial cells (Matthay and Zemans, 2011). Further

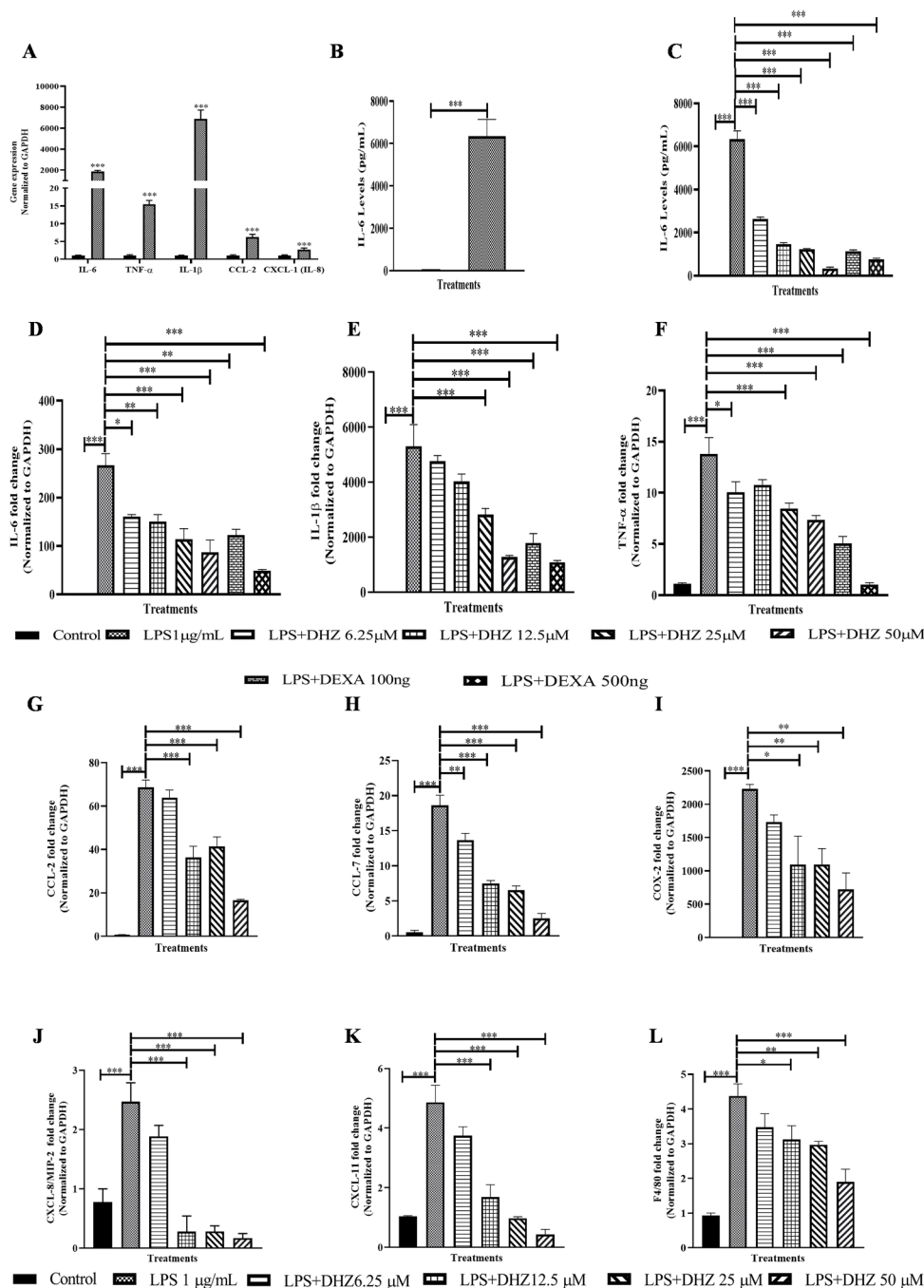


**Fig. 1.** DHZ treatment attenuates the LPS induced IL-6 gene expression in macrophages. RAW 264.7 cells were serum starved for 6 h then treated with or without LPS (1 μg/ml) for another 12 h. Thereafter, cell supernatant was harvested for ELISA for IL-6 estimation (A) and cells were harvested for RNA isolation and subjected to qRT-PCR analysis for the specified transcripts (B). RAW 264.7 cells were serum starved for 6 h then pre-treated with DHZ (6.25, 12.5, 25 and 50 μM) DEXA (100 ng/ml and 500 ng/ml), after 2 h, cells were treated with LPS (1 μg/ml) for another 12 h. Thereafter, cells were harvested for RNA isolation and subjected to qRT-PCR analysis for the IL-6 (B) and cell supernatant was harvested for ELISA for IL-6 estimation (C), further RT PCR was performed for specified primers (D–L). Graphs in panels represent fold change in gene expression normalized to β2M. Data represented as Mean ± SEM, n = 3. \*  $p < 0.05$ , \*\*  $p < 0.01$ , \*\*\*  $p < 0.001$ . NS, non-significant. (A) Two way and (B–L) One way ANOVA was performed for statistical analysis.

investigation was performed to check whether DHZ will show its similar biological activity in normal lung epithelial cells (BEAS-2B), and normal human endothelial cells (HUVEC). Before investigating the efficacy of DHZ, cell viability assay was performed, our results revealed DHZ did not show any cell death in the presence or absence of LPS at specified concentrations (Fig. S1E and F).

LPS challenge increased the pro-inflammatory cytokine and chemokine expression levels in BEAS-2B and (Fig. 2A–F), HUVEC cells (Fig. 2G and H). DHZ pre-treatment significantly attenuated the key inflammatory cytokine levels (IL-6, TNF-α, and IL-1β) as equal potency as DEXA (Fig. 2A–C). Further, DHZ significantly ( $p < 0.01$ ) mitigated the LPS induced expression levels of chemokines and Cox-2 in a dose-dependent manner in both the cell lines (Fig. 2D–H). In addition, we have validated the gene expression results by cytokine release with ELISA. DHZ treatment reduced the levels of inflammatory cytokines (IL-

6 and IL-8) significantly (Fig. 2I and J) compared to the LPS control. Overall, these results demonstrated that DHZ treatment mitigated the LPS induced cytokine and chemokine levels in a dose-dependent manner.

*DHZ mitigates LPS induced cell damage marker's expression in epithelial and endothelial cells*

To analyse whether DHZ, which was able to reduce inflammatory markers, could also protect the lung epithelial and endothelial cells from the LPS induced cell damage, we measured the LPS induced expression of alveolar pulmonary stretch (amphiregulin), epithelial cell damage (club cell protein 16 -CC16) markers in BEAS-2B and ICAM-1, VCAM-1 and amphiregulin in HUVEC cells in the presence or absence of DHZ. Gene expression data revealed that, LPS significantly ( $p < 0.01$ )

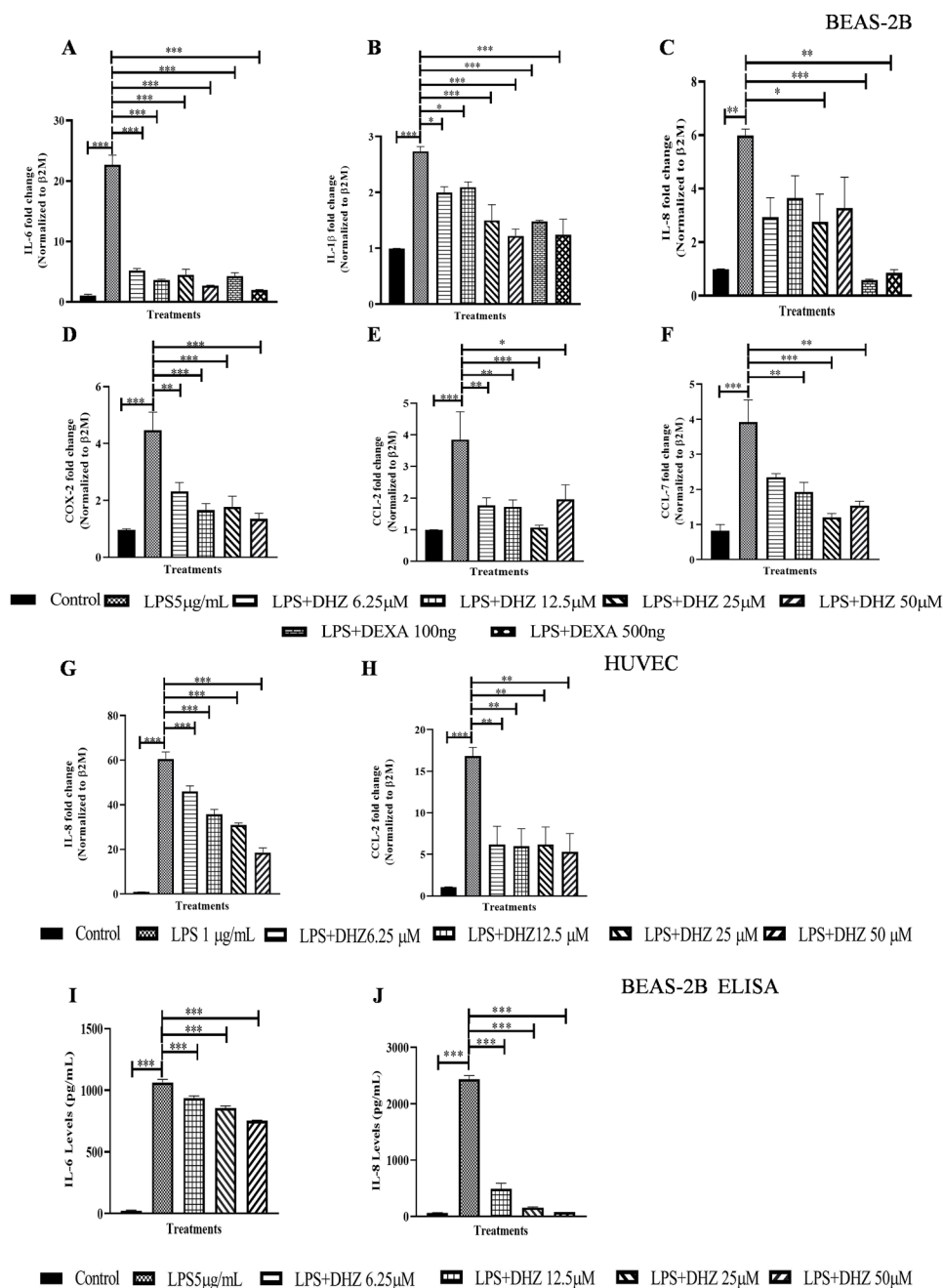


**Fig. 2.** DHZ reduces the inflammatory cytokine levels in epithelial and endothelial cells. BEAS-2B cells were pre-treated with DHZ (6.25, 12.5, 25 and 50  $\mu\text{M}$ ) and DEXA (100 ng/ml and 500 ng/ml), after 2 h, cells were treated with LPS (5  $\mu\text{g}/\text{ml}$ ) for another 12h. Thereafter, cells were harvested for RNA isolation and subjected to qRT-PCR analysis for the specified primers (A–F) and cell supernatant was harvested for performing the ELISA for IL-6 (I) and IL-8 (J). HUVEC cells were pre-treated with DHZ (6.25, 12.5, 25 and 50  $\mu\text{M}$ ) and after 2 h, cells were treated with LPS (1  $\mu\text{g}/\text{ml}$ ) for another 12 h. Thereafter, cells were harvested and subjected to qRT-PCR analysis for the specified primers (G and H) Graphs in panels represent fold change in gene expression normalized to  $\beta 2\text{M}$ . Data represented as Mean  $\pm$  SEM.,  $n = 3$ . \*  $p < 0.05$ , \*\*  $p < 0.01$ , \*\*\*  $p < 0.001$ . NS, non-significant. One way ANOVA was performed for statistical analysis.

enhanced the levels of cell injury markers in both the cell types, conversely DHZ treatment abolished the LPS induced alveolar pulmonary stretch and cell damage markers expression in BEAS-2B (Fig. 3A–D) and HUVEC cells in a dose-dependent manner (Fig. 3E–G).

#### DHZ reduces inflammatory pathway through inhibiting the oxidative stress, modulating the MAPK and NF- $\kappa\text{B}$ pathways

Emerging evidence suggests that ROS contribute to diverse signalling pathways, including the LPS-induced inflammatory signalling, for example, it was reported that TNF- $\alpha$  and IL-8 secretion can be inhibited by antioxidants (DeForge et al., 1992). To investigate the effect of DHZ on LPS induced ROS levels, RAW 264.7 (Fig. 4A and B) and BEAS-2B cells (Fig. 4C and D) were employed. In line with previous reports (Rao et al., 2011) on DHZ, our DCFDA analysis showed that LPS stimulation significantly increased the ROS levels, and DHZ treatment

significantly mitigated the ROS levels in a dose dependent-manner (Fig. 4A–D)

It is well known that multiple signalling pathways control the release of inflammatory cytokines and chemokines. One of the critical signalling pathways is the Mitogen-activated protein kinase (MAPK) pathway, comprising c-Jun amino-terminal kinases (JNK) and p38. To explain the mechanism by which DHZ exerts its anti-inflammatory effect, we measured the effects of DHZ on phosphorylation of JNK and p38 in RAW 264.7 cells. Western blot analysis revealed that LPS stimulated cells showed significant elevation of p-JNK, C-Jun and pp38 levels (Fig. 4E–H), whereas in the cells treated with DHZ significantly reduced the LPS induced phosphorylation of JNK, p38 and C-Jun levels in a dose-dependent manner (Fig. 4E–H).

Apart from the MAPK pathway, the NF- $\kappa\text{B}$  signalling transduction pathway plays a major role in the activation of inflammatory-related gene expression, which involves the phosphorylation and release of

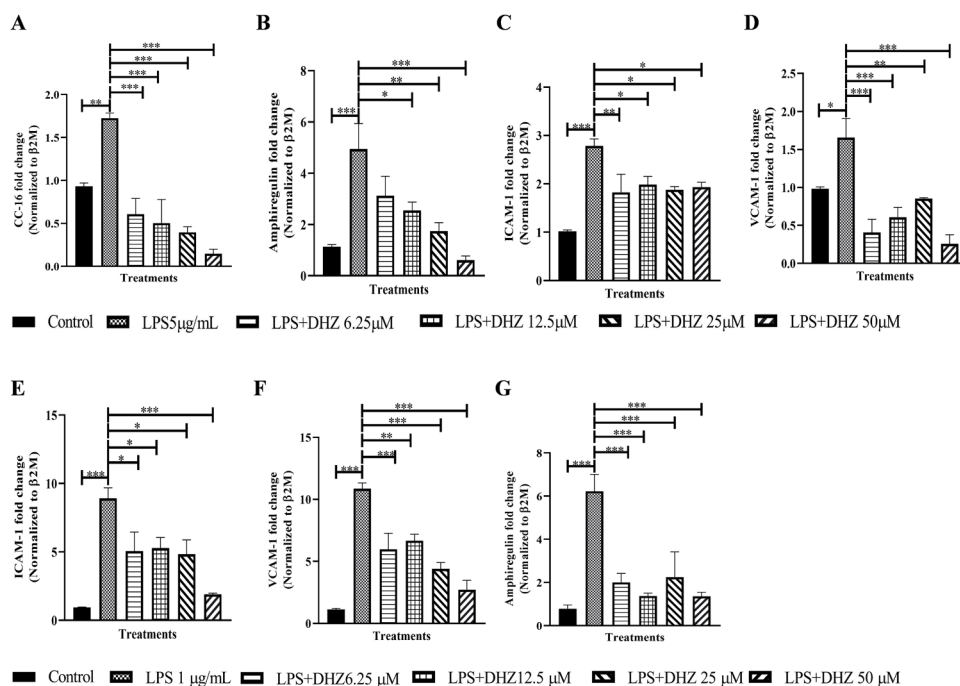


**Fig. 3.** DHZ mitigates LPS induced cell damage marker's expression in epithelial and endothelial cells.

BEAS-2B cells were pre-treated with DHZ (6.25, 12.5, 25 and 50 μM) and after 2 h, cells were treated with LPS (5 μg/ml) for another 12 h. Thereafter, cells were harvested for RNA isolation and subjected to qRT-PCR analysis for the specified primers (A–D). HUVEC cells were pre-treated with DHZ (6.25, 12.5, 25 and 50 μM) and after 2 h, cells were treated with LPS (1 μg/ml) for another 12 h. Thereafter, cells were harvested for RNA isolation and subjected to qRT-PCR analysis for the specified primers (E–G). Graphs in panels represent fold change in gene expression normalized to β2M. Data represented as Mean ± SEM, n = 3. \* p < 0.05, \*\* p < 0.01, \*\*\* p < 0.001. NS, non-significant. One way ANOVA was performed for statistical analysis.

IκB, phosphorylation of NF-κB and nuclear translocation (p65). Western blot analysis showed that increased phosphorylation of p65 and IκB-α in LPS stimulated cells, whereas, in the DHZ pre-treatment, these protein levels were decreased in a dose-dependent manner (Fig. 4E, I and J). Inconsistent with the above results, DHZ treatment reduced the phosphorylation of NF-κB and p38 protein in BEAS-2B cells (Fig. 4L–N).

Further, we focused on nuclear translocation of NF-κB, a marker of inflammatory signalling activation, using the RAW 264.7 cells. LPS stimulation significantly increased the translocation of NF-κB/p65 from the cytoplasm to nucleus (Fig. 4O–Q) which is inhibited by DHZ treatment. Overall, these results demonstrate that DHZ modulating MAPK and NF-κB signalling pathways.

MPO plays a typical role as a local mediator of tissue damage and resulting in activation of inflammation in various inflammatory disorders. These findings pinpoint, MPO as an important therapeutic target in the treatment of inflammatory conditions. Western blot analysis revealed that LPS stimulation significantly increased MPO levels and DHZ treatment mitigated the MPO levels in RAW 264.7 cells (Fig. 4E and K), therefore it suggests that DHZ may also exert its anti-oxidant action by regulating the MPO in inflammatory conditions.

Overall, these *in vitro* analyses demonstrated that DHZ treatment protected the lung cells by reducing the cytokine and chemokine expression levels and inflammatory mediated cellular damage via reducing the ROS levels by modulating the MAPK/NF-κB pathway.

#### DHZ treatment ameliorates the LPS induced physiological changes and inflammatory responses in rat lungs

To determine DHZ ability to protect lung injury in *in vivo*, we employed a rat model using the intratracheal installation of LPS. The effect of DHZ was assessed by measuring the body weight loss, index of the lung edema by estimating the lung wet/dry weight ratios, spleen index, haematological and BALF parameters in animals. LPS insult severely reduced the animal weight in both the time points (12 h and 24 h) and DHZ treatment significantly mitigated the LPS induced weight loss (Figs. 5A and S2). The lung wet/dry weight ratios and spleen indices were markedly increased in the LPS-control group than in the sham control, whereas in the DHZ treated groups lung wet/dry ratio was significantly reduced in both the time points (12 h and 24 h) (Figs. 5B, C

and S2B, C) suggesting improvement of lung condition upon DHZ treatment. Further, a significant reduction of spleen weight in DHZ treated rats were observed in 12 h time point, but not in 24 h animals.

It was reported that lung inflammation due to bacterial or viral infections results in increased inflammatory cells in the blood as well as in the BALF. In due course of ARDS development, the primed circulating neutrophils results in reduced deformability and increased retention within the pulmonary capillary bed, followed by migration into the airspaces by crossing the endothelium, interstitial and epithelial layers. The effect of DHZ on LPS induced infiltration of inflammatory cells in blood and as well as in BALF samples were investigated. Blood analysis revealed that immune-mediated cells such as neutrophils, lymphocytes and monocytes were significantly increased in LPS control animals compared to sham control (Figs. 5D, F, H, J, L, M and S2D, F, H, J, L, M). Interestingly, treatment with DHZ significantly attenuated the LPS induced inflammatory cells in blood samples (in 12 h and 24 h time point). On the other hand, BALF fluid analysis revealed that a significant (p < 0.001) increase in inflammatory cells in LPS control animals (Figs. 5E, G, I, K and S2E, G, I, K). In DHZ treated samples, significant reduction of WBC, neutrophil, lymphocytes and monocytes count was observed.

Further, the tissue damage markers such as ALP and LDH levels in BALF samples showed a significant (p < 0.01) increase in the LPS control, whereas upon DHZ treatment, both ALP (Figs. 5N and S2N) and LDH (Fig. S2O and S2O) levels were reduced. Overall, these results suggest that DHZ treatment mitigated the LPS induced infiltration of inflammatory cells and fluid accumulation in the lungs.

#### DHZ attenuated the LPS induced inflammatory cytokines in lung tissue homogenates and BALF samples

Previously, it was reported that elevated levels of various inflammatory cytokines were found in the BALF of ARDS patients who showed mortality (Meduri et al., 1995), suggesting a direct correlation between cytokine levels with the severity of ARDS. To investigate whether DHZ can control cytokine release, we employed a gene expression analysis in lung tissues and observed upregulation of proinflammatory (IL-6, TNF-α, IL-1β, IL-8/CXCL-1), inflammatory (COX-2) cytokine, chemokines and chemokine ligands (CXCL-10, CXCL-11, CCL2, CCL7, CXCL-6),

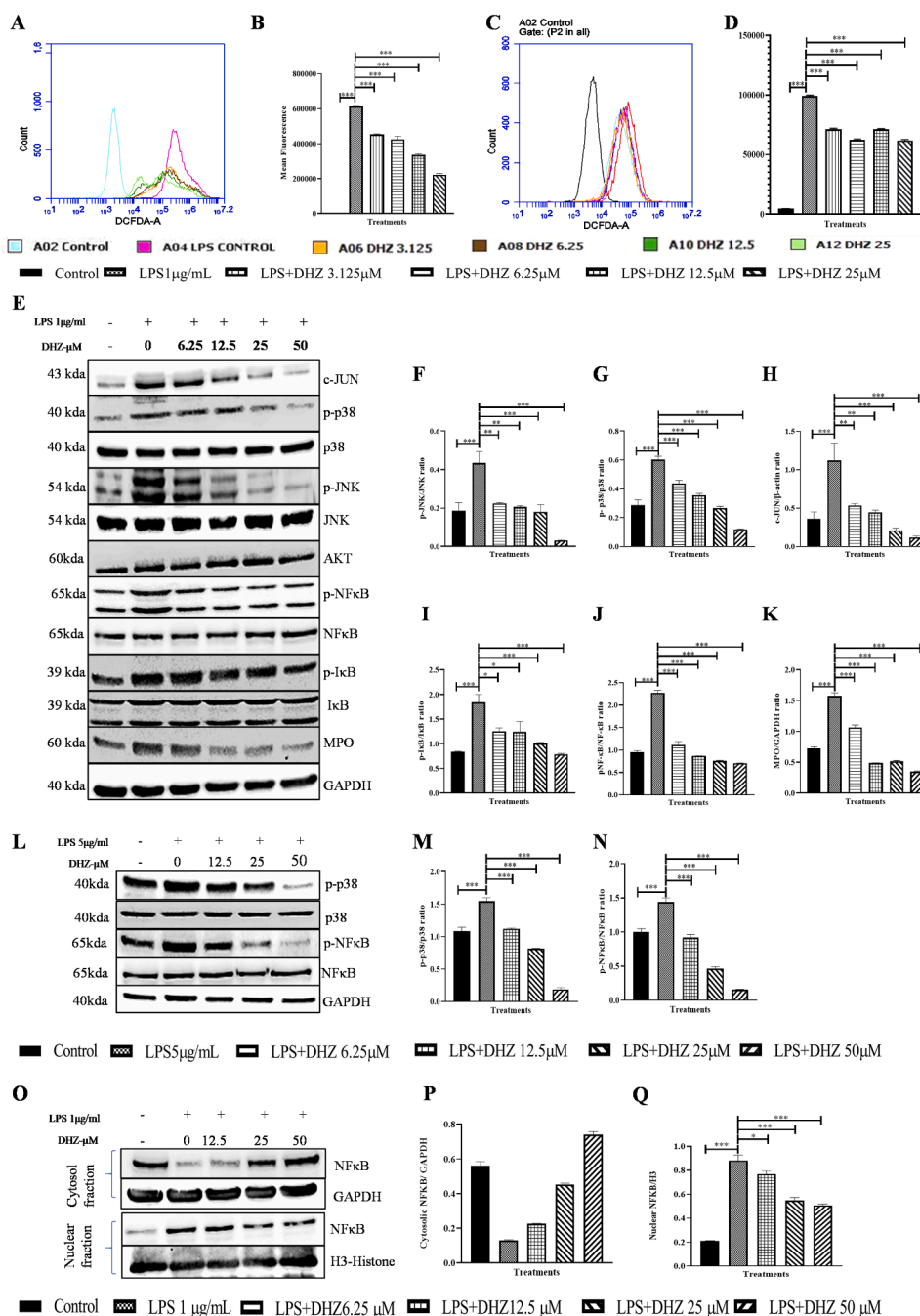


**Fig. 4.** DHZ reduces the inflammatory pathway through inhibiting the oxidative stress and modulating the MAPK and NF-κB pathways. RAW264.7 cells pre-treated with DHZ (6.25, 12.5, 25 and 50 μM) and after 2 h, cells were treated with LPS (1 μg/ml) for another 12 h. Thereafter, cells were trypsinized and subjected to DCFDA analysis using flow-cytometry (A and B). BEAS-2B cells were pre-treated with DHZ (6.25, 12.5, 25 and 50 μM) and after 2 h, cells were treated with LPS (1 μg/ml) for another 12 h. Thereafter, cells were trypsinized and subjected to DCFDA analysis using flow-cytometry (C and D). RAW264.7 cells were pre-treated with DHZ (6.25, 12.5, 25 and 50 μM) and after 2 h, cells were treated with LPS (1 μg/ml) for another 12 h. Thereafter, cells were harvested for protein isolation and subjected to western-blot analysis using specified antibodies (E). Protein expressions were quantified using image J software and graphs were plotted against each specified protein markers (F–K). BEAS-2B cells were pre-treated with DHZ (6.25, 12.5, 25 and 50 μM) and after 2 h, cells were treated with LPS (5 μg/ml) for another 12 h. Thereafter, cells were harvested for protein isolation and subjected to western-blot analysis using specified antibodies (L). Protein expressions were quantified using image J software and graphs were plotted against each specified protein markers (M and N). RAW264.7 cells were pre-treated with DHZ (6.25, 12.5, 25 and 50 μM) and after 2 h, cells were treated with LPS (1 μg/ml) for another 12 h. Thereafter, cells were harvested for cytoplasm and Nuclear protein isolation and subjected to western-blot analysis using specified antibodies (P). Protein expressions were quantified using image J software and graphs were plotted against each specified protein markers (P and Q). One way ANOVA was performed for statistical analysis.

and anti-inflammatory cytokine (IL-10) expression in LPS treated groups (Fig. 6A–L). DHZ treatment significantly reduced these proinflammatory cytokines and inflammatory (COX-2) cytokine (Figs. 6A–E and S3A–D), chemokines (Figs. 6F–J and S3E, F), and as well the concomitantly increased the IL-10 mRNA levels in treated samples compared to LPS control (Figs. 6L and S3H).

Further, BALF (Figs. 6M–P and S3I–L) and lung tissue homogenates (Fig. S3M–S) were subjected to pro-inflammatory cytokine analysis using ELISA. Consistent with the gene expression data, ELISA analysis resulted, significantly increased levels of cytokines (IL-6, IL-1β, IFN-γ and CCL2) in LPS control animals tissue homogenates and BALF samples. IL-10 cytokine levels were slightly elevated in LPS control. In the case of DHZ treated animal samples, we observed a significant reduction in the cytokine levels induced by LPS (Fig. S3M and R) and an increase in the IL-10 levels. Overall, these results suggest that DHZ significantly ( $p <$

0.01) attenuated the LPS induced cytokine expression (mRNA and protein) *in vivo* as observed in both lung tissues and BALF.

*Treatment with DHZ attenuated the LPS induced cytokine storm by inhibiting the oxidative stress and modulating the MAPK and NF-κB pathway*

Estimation of nitric oxide (NO) levels and western-blot analysis were performed to check whether DHZ exhibited a similar mode of action via reducing the NO levels, modulating the NF-κB and MAPK pathways in *in vivo*, as observed in *in vitro* experiments. Nitric oxide assay revealed that NO levels were significantly elevated in LPS control lung tissues and it was reduced in DHZ treated samples in a dose-dependent manner (Fig. 7A).

Western-blot analysis, from the animal tissues, revealed that LPS

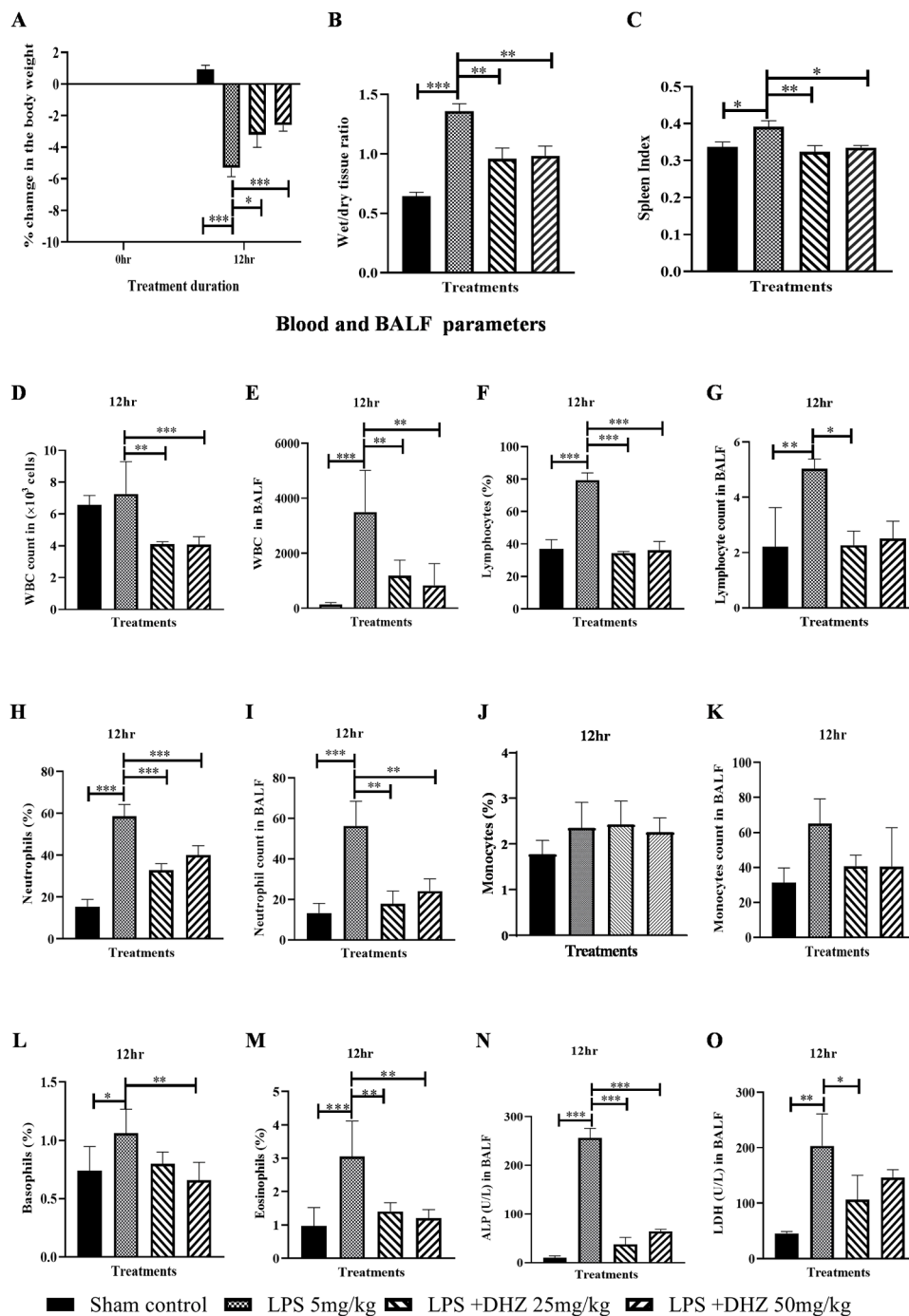


**Fig. 5.** DHZ treatment ameliorates the LPS induced physiological changes and inflammatory responses in rat lungs.

LPS Induced ARDS model was developed by intra-tracheal instillation of LPS (5 mg/kg) using male SD rats. Two hours after 5 mg/kg LPS instillation, rats were orally administered with two doses of DHZ (25 mg/kg) and DHZ (50 mg/kg) and vehicle control in disease control (LPS) groups and incubated for 12 h. After 12 h of the treatment, blood samples were collected from the 12-h time point group animals for cell counting analysis. After the specified incubation, animals were weighed to estimate the body weight loss (A), thereafter, were anesthetized and BALF fluid for cell counting and ELISA and lung tissue was collected for estimating the dry/wet ratio (B) and spleen was collected for spleen Index (C). Differential blood count analysis was performed to estimate the levels/percentage of following cells WBC (D), lymphocytes (F), Neutrophils (H), Monocytes (J), Basophils (L) and Eosinophils (M). Cell count analysis was performed in BALF samples to estimate the levels/percentage of WBC (E), lymphocytes (G), Neutrophils (I), Monocytes (K), Alkaline phosphatase (N) and lactate dehydrogenase (O). Data represented as Mean  $\pm$  SEM, n = 8. \*  $p < 0.05$ , \*\*  $p < 0.01$  vs. the LPS control group. A) Two way and B-O) One way ANOVA was performed for statistical analysis.

stimulation increased the phosphorylated forms of p-38, JNK and c-JUN levels, suggesting the activation of the MAPK pathway. On contrary, DHZ treatment reduced the phosphorylation of p-38, C-JUN and JNK levels (Fig. 7B, C and G). In addition to the MAPK pathway, the effect of DHZ on NF- $\kappa$ B pathway was also investigated, it was observed that LPS stimulation increased the I $\kappa$ B and p65 phosphorylation (Fig. 7B, E and F) in LPS control and treatment with DHZ mitigated the LPS induced phosphorylation of NF- $\kappa$ B in dose-dependent manner.

*DHZ treatment ameliorates the LPS induced infiltration of inflammatory cells, pathological changes and Neutrophil Extracellular Traps (NETs) in lung tissues*

Next, we investigated the ability of DHZ to protect the LPS induced

pathological changes in rat lung tissues by H&E analysis. Lung tissue sections from LPS control group showed a significant pathological alteration, including elevated peri-arteriolar inflammation with infiltrated inflammatory cells. Additionally, interstitial edema in alveolar spaces, accumulation of neutrophils in the alveolar spaces, alveolar inflammation and thickening of the alveolar wall was observed (Figs. 8A and S4A). In the DHZ treated lung sections, there was a remarkable reduction in tissue damage, edema in alveolar spaces, alveolar wall thickening, and alveolar inflammation was observed. DHZ treatment showed minimal peri-arteriolar inflammation with lower infiltration of inflammatory cells (neutrophils) in both the time points (Figs. 8A and S4A) of the treatment.

Excessive neutrophil elastase (NE) activity has been reported to cause tissue damage and interfere in remodelling processes in several

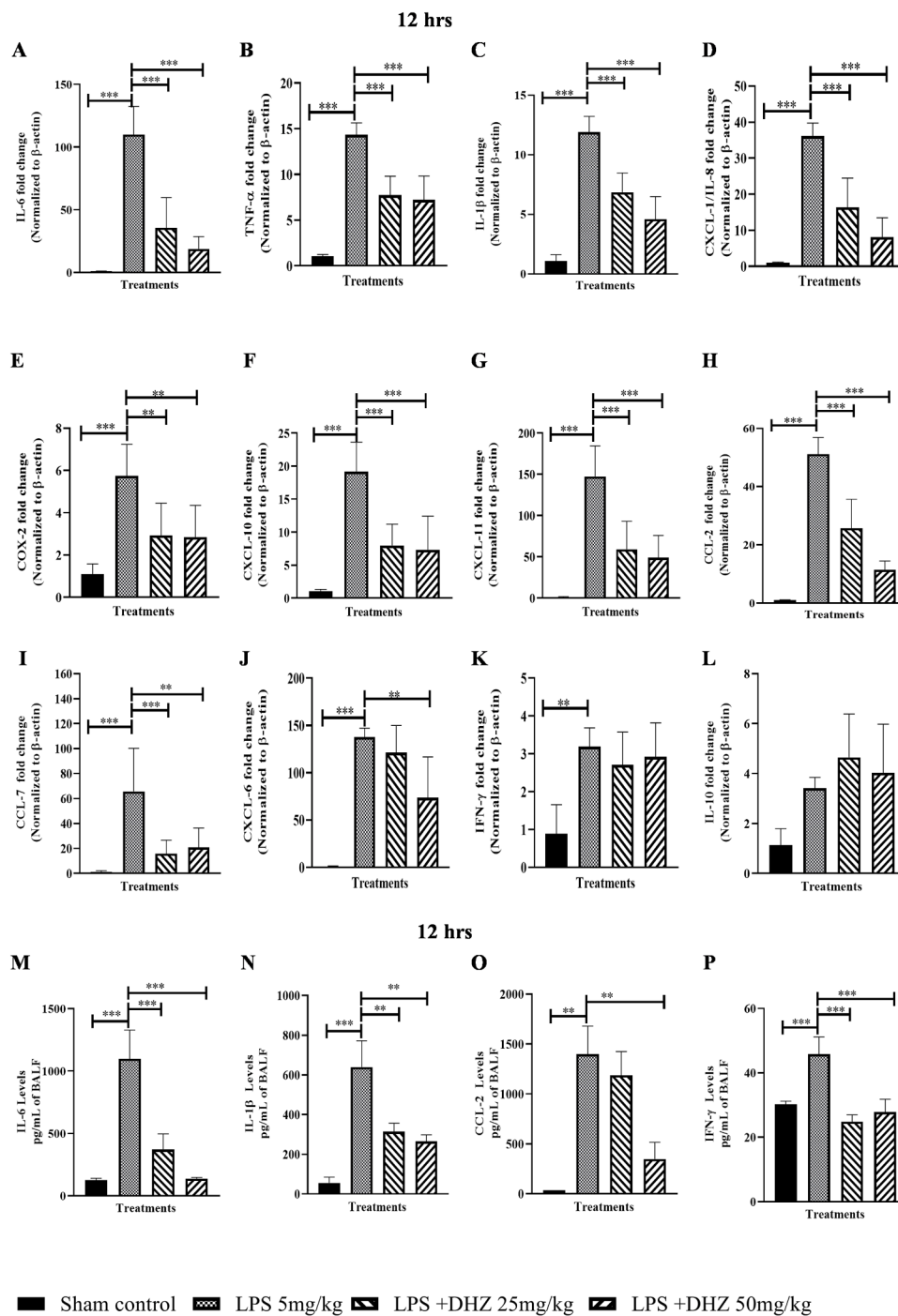


**Fig. 6.** DHZ attenuated the LPS induced inflammatory cytokines in lung tissue homogenates and BALF samples.

After 12 h of treatment, lung tissues were collected and part of tissues was subjected for Q-RT-PCR for the specified transcripts (A–L). After treatment, BALF samples were collected and part of sample was subjected to ELISA for the specified protein estimations (M–P). Data represented as Mean  $\pm$  SEM, n = 8. \*  $p < 0.05$ ; \*\*  $p < 0.01$ ; \*\*\*  $p < 0.001$  vs. the LPS control group. One way ANOVA was performed for statistical analysis.

clinical conditions such as pneumonia, respiratory distress, and ALI. Neutrophil infiltration is the hallmark of lung inflammation. To elucidate DHZ protective role in lung damage through neutrophil infiltration, we performed immune-histochemistry analysis for elastase, an enzyme released by neutrophils. Immunohistochemistry analysis revealed that enhanced elastase levels in LPS treated rat lung tissue specimens, whereas DHZ treatment showed a decrease in elastase expression (Fig. 8C and D). Since it was known that myeloperoxidase synergies with NE in driving chromatin de-condensation independent of its enzymatic activity in driving the lung damage, we analysed the expression of myeloperoxidase on the same tissue specimens. Interestingly, we

observed increased expression of myeloperoxidase in LPS treated lung specimens and treatment with DHZ reduced myeloperoxidase levels significantly (Fig. 8E and F). These results validated MPO results, which were obtained in western-blot analysis (Fig 7B and H). Further, to validate the cytokine/MPO/NE induced cellular damage, we investigated the apoptosis in tissue sections using TUNEL assay. TUNEL staining revealed that LPS stimulation significantly increased cell death in LPS control animals when compared to sham control. DHZ significantly reduced the cell death in a dose-dependent manner (Fig. 8G and H). Overall, histopathological and immuno-histochemistry analysis demonstrate that DHZ significantly ameliorated the LPS induced lung

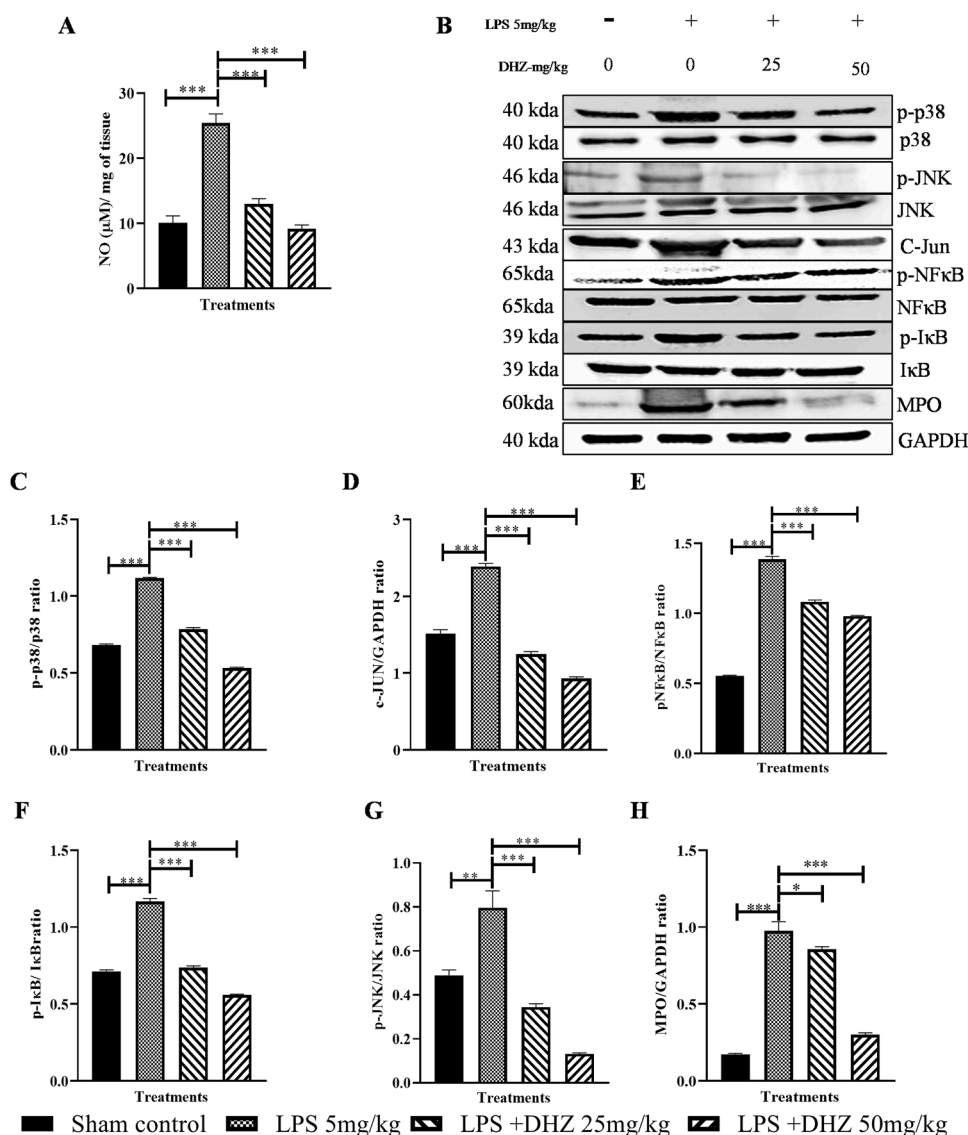


**Fig. 7.** Treatment with DHZ attenuated the LPS induced cytokine storm by inhibiting the oxidative stress and p-38 pathway.

After treatment, lung tissues were collected, and part of tissues were homogenized and subjected to nitric oxide estimation and other part of tissues were used to perform immunoblot analysis for the specified transcripts or antibodies respectively. (A) Nitric oxide estimation (B) Representative images of western blot. (C-G) Graph represents densitometric quantification of the specified proteins; Data represented as Mean  $\pm$  SEM, n = 8. \*  $p < 0.05$ ; \*\*  $p < 0.01$ ; \*\*\*  $p < 0.001$  vs. the LPS control group. One way ANOVA was performed for statistical analysis.

pathological abnormalities.

## Discussion

Often lung inflammation leads to cellular damage in ARDS model, the LPS induced cellular damage of lung endothelial and epithelial cells has been reported to play a significant role in the pathogenesis of ARDS (Bardales et al., 1996). In this study, we have demonstrated the anti-inflammatory activity of DHZ, a phytochemical, a half analogue of curcumin, in *in vitro* and *in vivo* models. Previously, it was reported that DHZ possesses anti-inflammatory activity mediated through its anti-oxidative property. Using the LPS- induced inflammatory *in vitro* model, we demonstrate a significant anti-inflammatory activity of DHZ in immune cells (RAW 264.7), human lung epithelial and endothelial cells. Dexamethasone and DHZ were able to reduce several inflammatory cytokines and chemokine significantly upon LPS stimulation. Generally, the lung is constantly challenged with various extracellular environmental agents for example chemical pollutants and pathological agents. Inflammation in the lungs is a complex process involving crosstalk between the inflammatory mediating macrophages, pulmonary epithelial and vascular endothelial cells (Robb et al., 2016). An ideal compound should work not only on immune cells but as well as on accessory cells. We report DHZ as a potential anti-inflammatory compound, which can

reduce LPS induced inflammation in macrophages and the epithelial and endothelial cells. It was shown that epithelial apoptosis is a key profibrotic event in lung fibrogenesis and involves modulation of the adhesion molecules (Janssen-Heininger et al., 2010). It was reported that pre-treatment with DHZ in HUVEC cells reduced the  $H_2O_2$ -induced ROS production and attenuated the adhesion molecule expression and secretion (Profumo et al., 2016). Increased expression levels of adhesion and cellular damage markers were observed in LPS challenged BEAS-2B and HUVEC cells which is consistent with the previous reports.

Our data also suggests that DHZ mediated the anti-inflammatory effect by blocking ROS production. It was previously shown that the airway epithelial and inflammatory cells contribute to ALI or ARDS through the activation of TLR signalling, cytokine and chemokine expression and as well as ROS generation (Qin et al., 2005). We found that LPS treatment induced a significant ( $p < 0.01$ ) elevation of ROS levels and these levels were mitigated in the presence of DHZ. Moreover, we have demonstrated that DHZ elucidates its anti-inflammatory effect through inhibition of the MAPKinase and NF- $\kappa$ B pathways. Chemical inhibitors blocking the NF- $\kappa$ B and MAP kinases are shown to play an important role as anti-inflammatory agents (Yamamoto and Gaynor, 2001). Activation of TLR signalling pathways is central to the release of cytokines through the activation of MAPK and NF- $\kappa$ B signalling. Phosphorylation of NF- $\kappa$ B, JNK and p38 proteins have been shown to play a

Histopathology 12 hrs

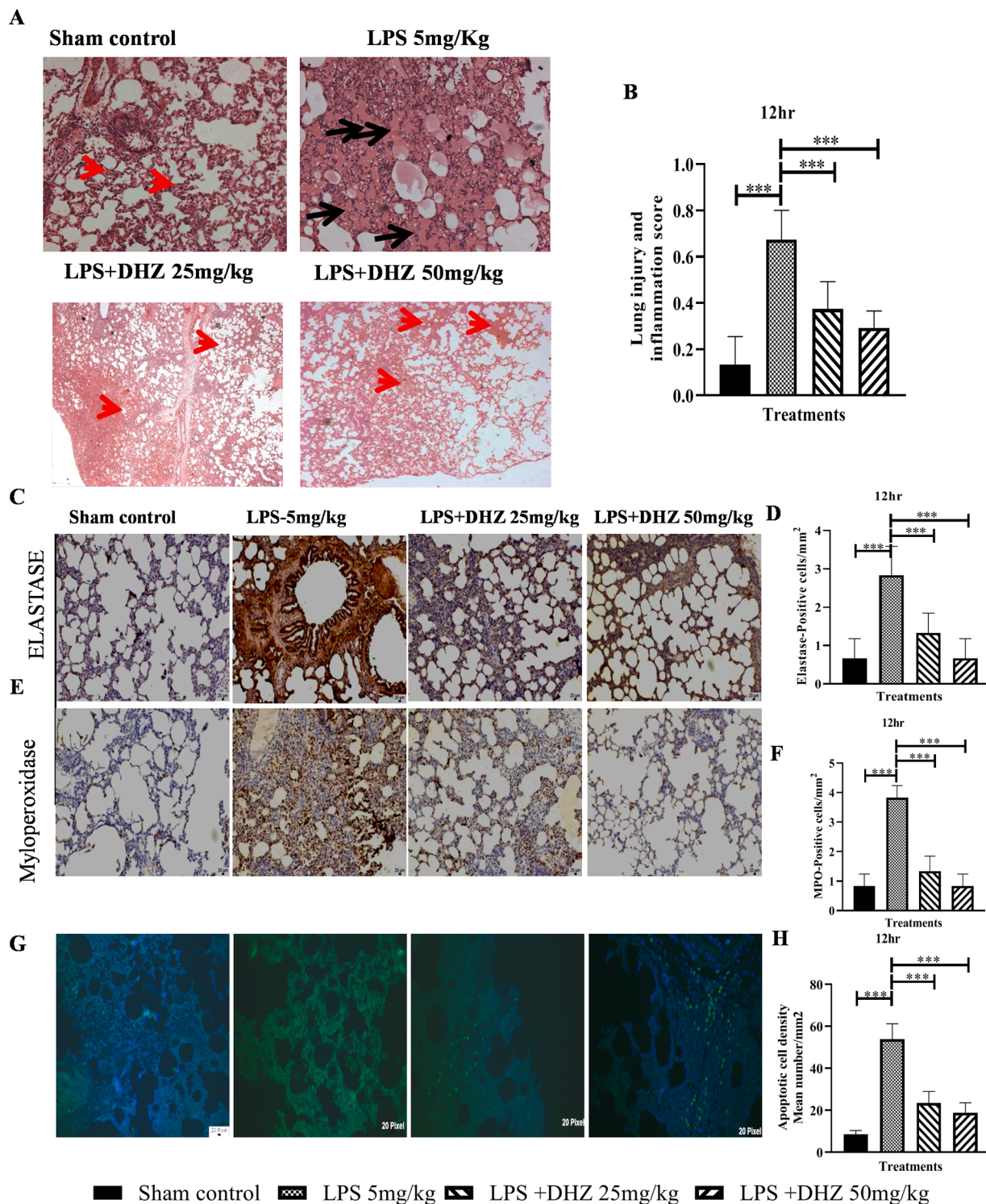


**Fig.8**

**Fig. 8.** DHZ treatment ameliorates the LPS induced infiltration of inflammatory cells, pathological changes and Neutrophil Extracellular Traps (NETs) in lung tissues. After treatment (12 h) with DHZ (25 mg/kg) or (50 mg/kg) or vehicle, lungs were isolated and subjected to histopathology and TUNEL assay. (A) Representative pictures (10 ×) of H&E-stained, The red arrow points at typical areas of inflammation, manifesting edema and infiltration of inflammatory cells. Graphs in panels represent the score of (B) lung injury and inflammation score. (C–F) Immunohistochemistry of Neutrophil elastase images (C) and quantification (D), Myeloperoxidase images (E) and quantification (F) in the lung sections. TUNEL assay images to identify the apoptotic cells (G) and quantification (H). Images were taken under original magnification × 20. Data represented as Mean ± SEM, n = 8 \* p < 0.05; \*\* p < 0.01; \*\*\* p < 0.001 vs. the LPS control group. One way ANOVA was performed for statistical analysis.

significant role in cytokine production and inflammation. It has been reported that NF- $\kappa$ B was activated in alveolar macrophages and tissue samples of ARDS patients (Moine et al., 2000). Our *in vitro* and *in vivo* results demonstrated that DHZ treatment significantly mitigated the LPS induced phosphorylation of p38, JNK and p65 proteins. We have clearly shown that DHZ was able to inhibit the phosphorylation of p65 and its nuclear translocation. Since, DHZ is a structural analogue of curcumin, which was known to be an antagonist of TLR4 signalling through inhibition of LPS-TLR4 complex formation (Molteni et al., 2018), hence we speculate that DHZ may elicit its inhibitory effect similarly by blocking the LPS-TLR4 complex formation.

In *in vivo*, several factors contributed to the pathogenesis of ARDS, including epithelial and endothelial interactions, neutrophil/macrophage associated responses, involvement of chemokine/cytokine expressions, coagulation abnormalities and surfactant imbalance (Matthay et al., 2019). LPS induced ARDS model replicates the cytokine storm event when we administer LPS through the intra-tracheal route. The anti-inflammatory effect of DHZ was further corroborated in *in vivo* rat ARDS model. Intratracheal injection of LPS resulted in increased inflammatory cell numbers in the lung as well as in the blood, as observed in human viral infections (for example SARS-CoV-2 infection). It was shown that dexamethasone mitigates the infiltration of inflammatory cells by inhibiting the NF- $\kappa$ B pathway (Fu et al., 2017). Treatment with DHZ post LPS insult attenuated the increase in inflammatory cells in lungs as seen in BALF and blood. BALF analysis revealed that DHZ treatment significantly reduced the LPS induced ALP and LDH levels, markers of acute and severe lung damage or infections. Consistent with the *in vitro* analysis, DHZ also reduced the inflammatory cytokine gene expression even in *in vivo* model.

Previous reports demonstrated that the CC chemokines CCL2 (MCP-1) and CCL7 (MCP-3), classical inflammatory monocyte chemokines, contribute to neutrophil recruitment in acute lung injury (Mercer et al., 2014). Consistently we have also observed a significant elevation of CCL2 and CCL7 in LPS control animals and DHZ treatment significantly reduced these chemokine levels. Neutrophil infiltration in the lungs is a classical marker for lung injury, which is known to be driven by CXC chemokines. Blockade of CXCL8/MIP-2 or CXCL1/2/IL-8 prevented neutrophil recruitment to some extent. In our study, we found that IL-8 expression was highly upregulated in LPS control and DHZ treatment significantly reduced its levels. These results were corroborated with the neutrophil count in BALF samples as well. DHZ also reduced the elevated cytokine and chemokine levels induced by LPS. It was previously reported that IL-6 and IL-8 levels were upregulated in BALF samples of ARDS patients (Schütte et al., 1996). LPS induced increase in inflammatory cells, edema in alveolar spaces, inflammation and cell death are mitigated by DHZ as evaluated by H&E analysis and TUNEL assay.

Mature neutrophils are known to elicit defence mechanisms to destroy invading pathogens by releasing various antimicrobial enzymes, including neutrophil elastase (NE), myeloperoxidase, matrix metalloproteinases, and cathelicidins (Hu et al., 2016). In case of infections, MPO and NE are rapidly discharged into phagosome vacuoles, where bacteria are trapped (Hirche et al., 2005). In inflammatory conditions, MPO and NE could leak out of the cell by several mechanisms and may inadvertently damage the host tissue (Olsson and Venge, 1980). NE contributes to the pathogenesis as well in the repair process of ALI and ARDS. Activated neutrophils use MPO to produce an array of potent toxic oxidants to induce oxidative stress that leads to cell death. It is known that MPO gets potentiated when NE levels reach high. Here we have shown that DHZ treatment significantly inhibited the MPO/NE levels in lung tissue samples indicating that, neutrophil extracellular traps were reduced in DHZ treatment. Dexamethasone is known to reduce the NE levels by TLR4 dependent pathway (Wan et al., 2017). This study also finds DHZ treatment significantly reduced the TLR 4 activated NE levels. Further TUNEL assay validated these results by showing reduced apoptotic cell density. These results extensively

demonstrated that DHZ may be a potential novel therapeutic anti-inflammatory agent against ALI/ARDS.

In humans, ALI/ARDS is associated with several risk factors like sepsis, oropharyngeal aspiration and comorbidities (Matute-Bello et al., 2008). LPS induced ALI animal models have a limitation in terms of replicating pathophysiology of human ALI. Moreover, animal models show variability in immunity and genetic parameters. In order to validate the protective ability of DHZ one may need to investigate on patient biopsies (*ex-vivo*) which may pave a path for the translational outcome.

## Conclusion

In conclusion, our study identifies a novel role for DHZ as a potent anti-inflammatory molecule in the alleviation of acute inflammation-induced ARDS and in the reduction of inflammation-mediated cytokine/chemokine production. DHZ demonstrates high efficacy by attenuating the IL-6, IL-1 $\beta$ , TNF- $\alpha$  and IL-8 levels in both *in vitro* and *in vivo*, and DHZ plays a critical role in mitigating the infiltration of inflammatory cells, neutrophil-mediated events and cellular damage in *in vivo* conditions. DHZ reduces levels of cytokines induced by LPS and attenuates measures of MAPK/Nf- $\kappa$ B signalling, suggesting that DHZ interferes with the inflammatory response to LPS. However, further investigation of functional evaluations of lung parameters may strengthen the protective effect of DHZ to position it as a therapeutic target against ARDS.

## Funding

This work was not funded.

## Authors' contribution

Conceptualization: S.B.A and S.R.K; Funding acquisition, Project administration, Resources: S.B.A and S.R.K; Investigation, Methodology: S.B.A, K.G, S.K.T; Validation, Visualization: S.B.A, K.G, MK, M.K.J, M.K, R.S.S.K and RK; Data curation, Formal analysis, Software: K.G, S.K.T; Supervision: S.R.K, Writing - original draft, Writing - review & editing: S. B.A, K.G, S.R.K;. All data were generated in-house, and no paper mill was used. All authors agree to be accountable for all aspects of work ensuring integrity and accuracy.

## Declaration of Competing Interest

The authors have no conflicts of interest in the submitted works.

## Acknowledgment

The authors are thankful to the Director, CSIR-IICT, Hyderabad, India, for providing facilities necessary for the completion of this work and his constant support. RK thanks the Council of Scientific and Industrial Research (CSIR), New Delhi, India, for the award of Junior Research Fellowship (JRF). CSIR-IICT manuscript communication number: IICT/Pubs/2021/019.

## Supplementary materials

Supplementary material associated with this article can be found, in the online version, at [doi:10.1016/j.phymed.2021.153729](https://doi.org/10.1016/j.phymed.2021.153729).

## References

- Amani, H., Shahbazi, M.-A., D'Amico, C., Fontana, F., Abbaszadeh, S., Santos, H.A., 2021. Microneedles for painless transdermal immunotherapeutic applications. *J. Control. Release* 330, 185–217.
- Andonegui, G., Zhou, H., Bullard, D., Kelly, M.M., Mullaly, S.C., McDonald, B., Long, E. M., Robbins, S.M., Kubes, P., 2009. Mice that exclusively express TLR4 on

- endothelial cells can efficiently clear a lethal systemic Gram-negative bacterial infection. *J. Clin. Invest.* 119, 1921–1930.
- Andugulapati, S.B., Gourishetti, K., Tirunavalli, S.K., Shaikh, T.B., Sistla, R., 2020a. Biochanin-A ameliorates pulmonary fibrosis by suppressing the TGF- $\beta$  mediated EMT, myofibroblasts differentiation and collagen deposition in *in vitro* and *in vivo* systems. *Phytomedicine* 78, 153298.
- Andugulapati, S.B., Gourishetti, K., Tirunavalli, S.K., Shaikh, T.B., Sistla, R., 2020b. Biochanin-A ameliorates pulmonary fibrosis by suppressing the TGF- $\beta$  mediated EMT, myofibroblasts differentiation and collagen deposition in *in vitro* and *in vivo* systems. *Phytomedicine* 78, 153298.
- Balaji, S.A., Udupa, N., Chamallamudi, M.R., Gupta, V., Rangarajan, A., 2016. Role of the drug transporter ABCB3 in breast cancer chemoresistance. *PLoS ONE* 11, e0155013.
- Bardales, R.H., Xie, S.S., Schaefer, R.F., Hsu, S.M., 1996. Apoptosis is a major pathway responsible for the resolution of type II pneumocytes in acute lung injury. *Am. J. Pathol.* 149, 845–852.
- Bosch, A.A.T.M., Biesbroek, G., Trzcinski, K., Sanders, E.A.M., Bogaert, D., 2013. Viral and bacterial interactions in the upper respiratory tract. *PLoS Pathog.* 9, e1003057-e1003057.
- Chibber, P., Kumar, C., Singh, A., Assim Haq, S., Ahmed, I., Kumar, A., Singh, S., Vishwakarma, R., Singh, G., 2020. Anti-inflammatory and analgesic potential of OA-DHZ; a novel semisynthetic derivative of dehydrozingerone. *Int. Immunopharmacol.* 83, 106469.
- DeForge, L.E., Fantone, J.C., Kenney, J.S., Remick, D.G., 1992. Oxygen radical scavengers selectively inhibit interleukin 8 production in human whole blood. *J. Clin. Invest.* 90, 2123–2129.
- Erickson, S., Schibler, A., Numa, A., Nuthall, G., Yung, M., Pascoe, E., Wilkins, B., 2007. Acute lung injury in pediatric intensive care in Australia and New Zealand: a prospective, multicenter, observational study. *Pediatr. Crit. Care Med.* 8, 317–323.
- Fu, P.K., Yang, C.Y., Huang, S.C., Hung, Y.W., Jeng, K.C., Huang, Y.P., Chuang, H., Huang, N.C., Li, J.P., Hsu, M.H., Chen, J.K., 2017. Evaluation of LPS-induced acute lung injury attenuation in rats by aminothiazole-paeonol derivatives. *Molecules* 22 (10):1605.
- Hirche, T.O., Gaut, J.P., Heinecke, J.W., Belaouaj, A., 2005. Myeloperoxidase plays critical roles in killing *Klebsiella pneumoniae* and inactivating neutrophil elastase: effects on host defense. *174*, 1557–1565.
- Hu, S.C.-S., Yu, H.-S., Yen, F.-L., Lin, C.-L., Chen, G.-S., Lan, C.-C.E., 2016. Neutrophil extracellular trap formation is increased in psoriasis and induces human  $\beta$ -defensin-2 production in epidermal keratinocytes. *Sci. Rep.* 6, 31119.
- Hung, I.F., Lung, K.C., Tso, E.Y., Liu, R., Chung, T.W., Chu, M.Y., Ng, Y.Y., Lo, J., Chan, J., Tam, A.R., Shum, H.P., Chan, V., Wu, A.K., Sin, K.M., Leung, W.S., Law, W. L., Lung, D.C., Sin, S., Yeung, P., Yip, C.C., Zhang, R.R., Fung, A.Y., Yan, E.Y., Leung, K.H., Ip, J.D., Chu, A.W., Chan, W.M., Ng, A.C., Lee, R., Fung, K., Yeung, A., Wu, T.C., Chan, J.W., Yan, W.W., Chan, W.M., Chan, J.F., Lie, A.K., Tsang, O.T., Cheng, V.C., Que, T.L., Lau, C.S., Chan, K.H., To, K.K., Yuen, K.Y., 2020. Triple combination of interferon beta-1b, lopinavir-ritonavir, and ribavirin in the treatment of patients admitted to hospital with COVID-19: an open-label, randomised, phase 2 trial. *Lancet* 395, 1695–1704.
- Janssen-Heininger, Y.M.W., Aesif, S.W., van der Velden, J., Guala, A.S., Reiss, J.N., Roberson, E.C., Budd, R.C., Reynaert, N.L., Anathy, V., 2010. Regulation of apoptosis through cysteine oxidation: implications for fibrotic lung disease. *Ann. N. Y. Acad. Sci.* 1203, 23–28.
- Kim, I.S., Yang, E.J., Shin, D.H., Son, K.H., Park, H.Y., Lee, J.S., 2014. Effect of arazyme on the Lipopolysaccharide-induced inflammatory response in human endothelial cells. *Mol. Med. Rep.* 10, 1025–1029.
- Liu, B., Li, M., Zhou, Z., Guan, X., Xiang, Y., 2020. Can we use interleukin-6 (IL-6) blockade for coronavirus disease 2019 (COVID-19)-induced cytokine release syndrome (CRS)? *J. Autoimmun.* 111, 102452.
- Liu, Y., Liu, B., Zhang, G.-q., Zou, J.-f., Zou, M.-l., Cheng, Z.-s., 2018. Calpain inhibition attenuates bleomycin-induced pulmonary fibrosis via switching the development of epithelial-mesenchymal transition. *Naunyn-Schmiedeberg's Arch. Pharmacol.* 391, 695–704.
- Matthay, M.A., Zemans, R.L., 2011. The acute respiratory distress syndrome: pathogenesis and treatment. *Annu. Rev. Pathol.* 6, 147–163.
- Matthay, M.A., Zemans, R.L., Zimmerman, G.A., Arabi, Y.M., Beitler, J.R., Mercat, A., Herridge, M., Randolph, A.G., Calfee, C.S., 2019. Acute respiratory distress syndrome. *Nat. Rev. Dis. Primers* 5, 18.
- Matute-Bello, G., Frevert, C.W., Martin, T.R., 2008. Animal models of acute lung injury. *Am. J. Physiol. Lung Cell. Mol. Physiol.* 295, L379–L399.
- Meduri, G.U., Headley, S., Kohler, G., Stentz, F., Tolley, E., Umberger, R., Leeper, K., 1995. Persistent elevation of inflammatory cytokines predicts a poor outcome in ARDS. Plasma IL-1 beta and IL-6 levels are consistent and efficient predictors of outcome over time. *Chest* 107, 1062–1073.
- Mercer, P.F., Williams, A.E., Scotton, C.J., José, R.J., Sulikowski, M., Moffatt, J.D., Murray, L.A., Chambers, R.C., 2014. Proteinase-activated receptor-1, CCL2, and CCL7 regulate acute neutrophilic lung inflammation. *Am. J. Respir. Cell Mol. Biol.* 50, 144–157.
- Moine, P., McIntyre, R., Schwartz, M.D., Kaneko, D., Shenkar, R., Le Tulzo, Y., Moore, E. E., Abraham, E., 2000. NF-kappaB regulatory mechanisms in alveolar macrophages from patients with acute respiratory distress syndrome. *Shock* 13, 85–91.
- Molteni, M., Bosi, A., Rossetti, C., 2018. Natural products with toll-like receptor 4 antagonist activity. *Int. J. Inflamm.* 2018, 2859135.
- Olsson, I., Venge, P., 1980. The role of the human neutrophil in the inflammatory reaction. *Allergy* 35, 1–13.
- Profumo, E., Buttari, B., D'Arcangelo, D., Tinaburri, L., Dettori, M.A., Fabbri, D., Delogu, G., Riganò, R., 2016. The nutraceutical dehydrozingerone and its dimer counteract inflammation- and oxidative stress-induced dysfunction of *in vitro* cultured human endothelial cells: a novel perspective for the prevention and therapy of atherosclerosis. *Oxid. Med. Cell Longev.* 2016, 1246485–1246485.
- Qin, L., Li, G., Qian, X., Liu, Y., Wu, X., Liu, B., Hong, J.S., Block, M.L., 2005. Interactive role of the toll-like receptor 4 and reactive oxygen species in LPS-induced microglia activation. *Glia* 52, 78–84.
- Rao, M.C., Sudheendra, A.T., Nayak, P.G., Paul, P., Kutty, G.N., Shenoy, R.R., 2011. Effect of dehydrozingerone, a half analog of curcumin on dexamethasone-delayed wound healing in albino rats. *Mol. Cell. Biochem.* 355, 249–256.
- Robb, C.T., Regan, K.H., Dorward, D.A., Rossi, A.G., 2016. Key mechanisms governing resolution of lung inflammation. *Semin. Immunopathol.* 38, 425–448.
- Rubinfeld, G.D., Caldwell, E., Peabody, E., Weaver, J., Martin, D.P., Neff, M., Stern, E.J., Hudson, L.D., 2005. Incidence and outcomes of acute lung injury. *N. Engl. J. Med.* 353, 1685–1693.
- Salgado, A., Bóveda, J.L., Monasterio, J., Segura, R.M., Mourelle, M., Gómez-Jiménez, J., Peracaula, R., 1994. Inflammatory mediators and their influence on haemostasis. *Haemostasis* 24, 132–138.
- Schütte, H., Lohmeyer, J., Rosseau, S., Ziegler, S., Siebert, C., Kielisch, H., Pralle, H., Grimminger, F., Morr, H., Seeger, W., 1996. Bronchoalveolar and systemic cytokine profiles in patients with ARDS, severe pneumonia and cardiogenic pulmonary oedema. *Eur. Respir. J.* 9, 1858–1867.
- Silva, P.L., Pelosi, P., Rocco, P.R.M., 2020. Personalized pharmacological therapy for ARDS: a light at the end of the tunnel. *Investig. Drugs* 29, 49–61.
- Tetz, L.M., Kamau, P.W., Cheng, A.A., Meeker, J.D., Loch-Carus, R., 2013. Troubleshooting the dichlorofluorescein assay to avoid artifacts in measurement of toxicant-stimulated cellular production of reactive oxidant species. *J. Pharmacol. Toxicol. Methods* 67, 56–60.
- Wan, T., Zhao, Y., Fan, F., Hu, R., Jin, X., 2017. Dexamethasone inhibits *S. aureus*-induced neutrophil extracellular pathogen-killing mechanism, possibly through toll-like receptor regulation. *Front. Immunol.* 8, 60.
- Yamamoto, Y., Gaynor, R.B., 2001. Therapeutic potential of inhibition of the NF-kappaB pathway in the treatment of inflammation and cancer. *J. Clin. Invest.* 107, 135–142.
- Yogosawa, S., Yamada, Y., Yasuda, S., Sun, Q., Takizawa, K., Sakai, T., 2012. Dehydrozingerone, a structural analogue of curcumin, induces cell-cycle arrest at the G2/M phase and accumulates intracellular ROS in HT-29 human colon cancer cells. *J. Nat. Prod.* 75, 2088–2093.